Mining, Metallurgy & Exploration (2019) 36:1091–1099
https://doi.org/10.1007/s42461-019-00108-5

Dissolution Kinetics Potential of a Biotite-Rich Kaolinite Ore for Industrial Applications by Oxalic Acid Solution

Alafara A. Baba[1] · Mustapha A. Raji[1] · Aishat Y. Abdulkareem[1,2] · Malay K. Ghosh[3] · Rafiu B. Bale[4] · Christianah O. Adeyemi[1,5]

Received: 11 October 2018 / Accepted: 1 July 2019 / Published online: 9 July 2019

Abstract
The increasing demand for pure aluminum and aluminum compounds of industrial quality from kaolinite ore cannot be overemphasized. Nigeria is one of the African countries endowed with abundant solid mineral resources that have not been sufficiently exploited to assist its indigenous industries. A wide array of applications of pure aluminum and its compounds are available, such as paper filling, refractories, adsorbent, catalysis, and paint additives. In this study, the upgrading of a Nigerian biotite-rich kaolinite ore by a hydrometallurgical route was investigated in oxalic acid media. During leaching studies, the effects of parameters including reaction temperature, lixiviant concentration and particle size on the extent of ore dissolution were examined. At optimal conditions (1.0 mol/L $C_2H_2O_4$, 75 °C), 92.0% of the initial 10 g/L ore was reacted within 120 min. The dissolution curves from the shrinking core model were analyzed and found to conform to the assumption of surface diffusion reaction, and the calculated activation energy of 33.2 kJ/mol supported the proposed model. The unreacted product (~8.0%) analyzed by XRD was found to contain siliceous impurities and could serve as a valuable by-product for certain industries.

Keywords Biotite-rich kaolinite ore · Nigeria · Oxalic acid · Leaching · Reaction mechanism

1 Introduction

Recent years have seen increasing demand for pure aluminum and aluminum compounds of industrial value from kaolinite ore and varieties [1–3]. Kaolinite ($Al_2Si_2O_5(OH)_4$) made of silica (SiO_4) tetrahedral sheets and gibbsite ($AlO_2(OH)_4$) octahedral sheets with a 1:1 alternating arrangement, is an important industrial mineral with unique properties that include small surface area, low cation exchange capacity, platelet particle structure, and inertness [4–6]. These properties make it suitable for numerous industrial applications, particularly as paper filling and coating, refractories, ceramics, extender, cement, catalysis, adsorbents, paints, plastics, rubber and for other defined polymeric uses [7]. In all of these, the extent of whiteness and brightness indexes are the most important parameters for specific consideration of the suitability of pure kaolinite for various industrial applications.

However, continuous efforts are needed to improve the ore whiteness index by removing the proximate impurities that may have an adverse effect on its industrial usage. For example, depending on the nature of kaolinite variety, impurities which often have an adverse effect on industrial ore quality and thus must be treated include quartz, anatase, feldspar and iron [8]. These are expressed as segregate phases or combined in the kaolinite lattice. Of these impurities, iron often constitutes the major impurity in the kaolin ore body. Iron can be removed by several methods such as physical separation: flotation or magnetic separation, or by leaching with suitable leachants including organic/inorganic acids. For example, hydrochloric acid (HCl), oxalic acid ($C_2H_2O_4$), sodium dithionite ($Na_2S_2O_3$) and phosphoric acid (H_3PO_4) are widely used in kaolinite ore processing to improve its industrial utility [9]. Titanium dioxide, the second most common mineral

✉ Alafara A. Baba
baalafara@yahoo.com; alafara@unilorin.edu.ng

✉ Mustapha A. Raji
mustaphaadekunle48@gmail.com

[1] Department of Industrial Chemistry, University of Ilorin, P.M.B. 1515, Ilorin 240003, Nigeria

[2] National Mathematical Centre, P.M.B. 118, Sheda Kwali, Abuja, Nigeria

[3] CSIR-Institute of Minerals and Materials Technology, Bhubaneswar 751013, India

[4] Department of Geology and Mineral Sciences, University of Ilorin, P.M.B. 1515, Ilorin 240003, Nigeria

[5] Department of Science Laboratory Technology, Federal Polytechnic Offa, P.M.B. 420, Offa, Nigeria

impurity found in kaolin, usually occurs in three modifications: anatase, brookite and rutile [10]. Researchers have focused on alternative routes of purification via bioleaching processes using heterotrophic bacteria such as *Thiobacillus ferrooxidans* [11–13]. However, there are many unresolved problems regarding the fitness of such processes for industrial use due to the microorganisms and the contaminants that may be associated with it. For this reason, and because of its bleaching power, oxalic acid is efficient and a better candidate for removal of iron and other impurities from the kaolin ore body, and is currently applied to improve the whiteness index for added industrial value [14]. This leachant has been found to moderately enhance the intercalation and attrition of the substrates at defined optimal leaching conditions, in terms of porosity, surface area and number of active sites [15].

Therefore, in light of the high bleaching strength of oxalic acid leachant, and given the limited data currently available regarding its use in the treatment of Nigerian kaolin ore varieties [16] for added industrial value, this study was initiated to explore its potential use. Biotite-rich kaolinite ore is widely distributed with proven reserves in some Nigerian states, with few efforts toward mining it for metallurgical uses thus far. Thus, it is our hope that the data obtained in this study will be utilized for predicting a possible pathway for upgrading the ore for defined industrial applications.

2 Materials and Method

2.1 Materials

The biotite-rich kaolinite ore used for this investigation was sourced from Nane Didan Bundugu area (longitudes 12°03 46.5 N and latitudes 06°29 77 E), Zamfara State, Nigeria. The ore was ground and sieved using the American Standard Test Method (ASTM) to four particle sizes: −75 + 45 μm, −90 +63 μm, −112 +90 μm and − 134 +107 μm. The finest particle size of −75 +45 μm, assumed to have a larger surface area unless otherwise stated, was used for all the dissolution experiments in this study. Deionized water was used to prepare all aqueous solutions.

2.2 Physicochemical Tests

2.2.1 Moisture Content (MC)

In the assessment of dryness or otherwise, 5.0 g of biotite-rich kaolinite ore was weighed into a crucible and oven-dried for 5 h. The sample was removed and transferred immediately into the desiccator to cool in order to prevent atmospheric moisture interference. The ore was re-weighed and the difference in weight was recorded. The MC tests were carried out in triplicate and the results were averaged [17].

2.2.2 Loss of Mass on Ignition (LOMOI)

In this test, 5.0 g of the ore was weighed into a crucible and kept in a muffle furnace for 2 h. The crucible was removed and transferred into a desiccator to cool, and the sample was re-weighed. The test was performed in triplicate, as the results taken as percentage LOMOI [17].

2.2.3 pH Determination

Twenty grams of the finest particle size (−75 +45 μm) was dissolved in distilled water and thoroughly stirred. The pH of the aqueous suspension was determined using a HANNA Model 215 pH meter. Measurement of the pH of the aqueous suspension was also carried out in triplicate [17].

2.3 Leaching Procedure

Leaching experiments were conducted in a 600 ml Pyrex glass reactor equipped with a thermometer to control the temperature and a stirrer to homogenize the solution. A 10 g/L sample of the pulverized ore was added to the prepared solution at a predetermined leachant concentration at a specified temperature. The fraction of ore dissolved with respect to the mass of the sample was varied at various time intervals (5 to 120 min) and at various oxalic acid ($C_2H_2O_4$) concentrations (0.1–1.5 mol/L). The leaching solution withdrawn was filtered and analyzed. The loss in weight of the sample during leaching was calculated by the difference, and the amount of aluminum in the leachate was spectrophotometrically determined; iron and other metals present in the leach liquor were estimated using a Buck Scientific Accusys 211 atomic absorption spectrophotometer. The concentration that gave the highest fraction dissolved was used for the optimization of other parameters including reaction temperature and particle size variations. Also, from the relevant Arrhenius relations, the activation energy, Ea, and Arrhenius constants were obtained to gain a better understanding and prediction of the dissolution mechanism for subsequent use in solvent extraction investigations [18]. The residual product at optimal leaching conditions was analyzed using X-ray diffraction (XRD), energy-dispersive X-ray spectroscopy (EDS) and scanning electron microscopy (SEM) analyses for material purity tests. The leaching process previously reported is consistent with the following stoichiometry [19, 20]:

During the ore dissolution, oxalic acid ($C_2H_2O_4$) dissociates to produce bi-oxalate ion ($HC_2O_4^-$):

$$C_2H_2O_4 \rightarrow H^+ + HC_2O_4^-, \quad (1)$$

and thus releases the oxalate ion ($C_2O_4^{2-}$):

$$HC_2O_4^- \rightarrow H^+ + C_2O_4^{2-}, \quad (2)$$

forming bi-oxalate ion, which reacts and possibly masks iron and other impurities (Eq. 3) in the solution, leaving aluminum ion as the major species.

$$Fe_2O_3 + H^+ + 5HC_2O_4^- \rightarrow 2Fe(C_2O_4)_2^{2-} + 3H_2O + 2CO_2 \quad (3)$$

3 Results and Discussion

3.1 Physicochemical Studies

The percentage of the ore moisture content gave 0.53 ± 0.041%. This result is in good accord with some other literature values. However, this value is lower than those from Rio Maior and Somical, Portugal, where their humidity content yielded 1.60 and 0.77%, respectively. The difference in data from the two Portuguese cities (Rio Maior and Somical) compared with the value obtained in this study could be due to the nature of the ore, topography, or environmental or geographical conditions [15, 17].

The resulting percentage weight of the volatile compounds in the biotite-rich kaolinite mineral after ignition was 13.3 ± 0.01%, almost the same as samples from the two Portuguese cities (Rio Maior and Somical), where 13.21% was recorded as the percentage LOMOI [17, 21].

The pH value of the aqueous suspension recorded for the ore under study was 6.05. This showed that the surface of the ore body is slightly acidic. Similarly, pH 5.35 and 4.50 were previously obtained from other ore sources [17].

3.2 Ore Characterization

The chemical analysis of the biotite-rich kaolinite ore, as examined using a PANalytical MiniPal energy dispersive X-ray fluorescence spectrometer, gave SiO_2 (23.98%), Fe_2O_3 (8.59%), Al_2O_3 (3.76%), K_2O (2.59%) and MnO_2 (0.03%), respectively. As examined by EDS, the raw ore gave oxygen (42.34%), aluminum (2.62%), silicon (13.44%), iron (1.97%), and carbon (38.61%), with sulfur and titanium occurring from low to minute levels (≤ 1%). The XRD results showed that *kaolinite* ($Al_{2.00}Si_{2.00}O_{9.00}$: 96-900-9231), *biotite* ($Mg_{6.55}Fe_{3.46}Al_{5.29}Ti_{1.34}Si_{11.36}K_{4.00}O_{48.00}$: 96-900-0844) and *quartz* ($Si_{3.00}O_{6.00}$: 96-900-9667) were the major compounds present in the ore. Other compounds detected in low to trace levels (≤1%) were rutile (TiO_2: 14-85450-1667) and hematite (Fe_2O_3: 71-1460-2841). The parent ore structure was examined with an FEI Nova NanoSEM 230 analyzer equipped with an emission gun at 5000 magnification, which confirmed that the kaolinite ore under study consisted of large particles stacked together to form agglomerates (Fig. 1) [22].

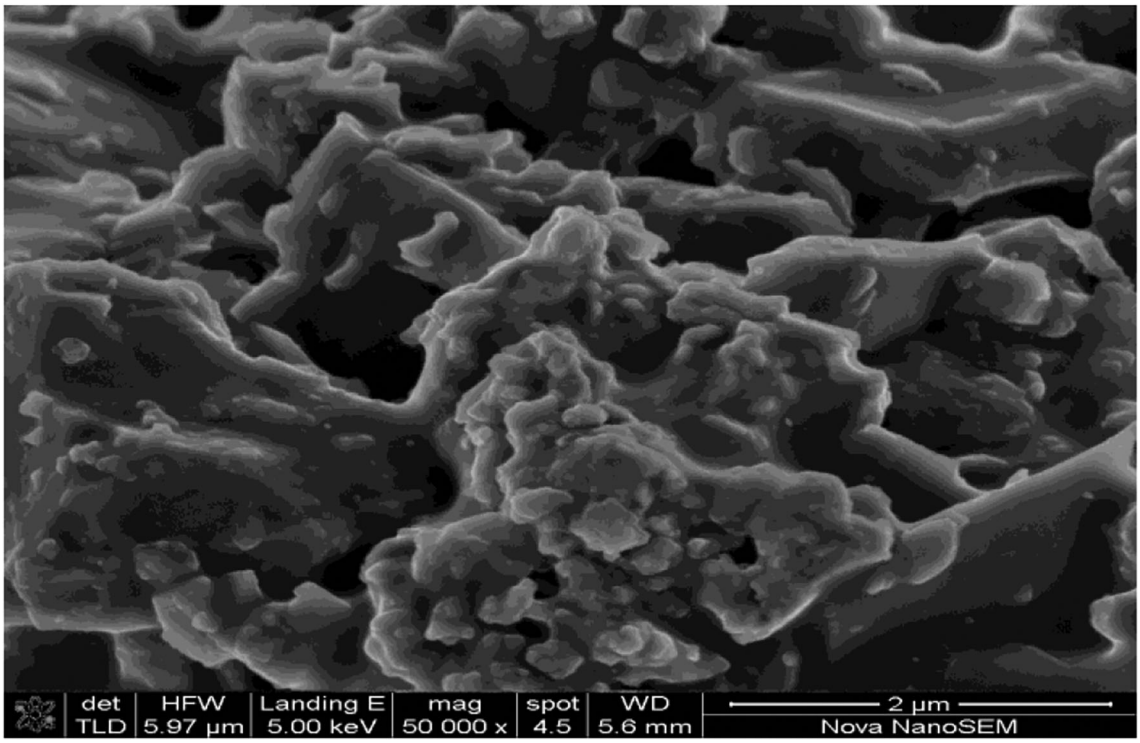

Fig. 1 SEM micrograph of raw biotite-rich kaolinite mineral

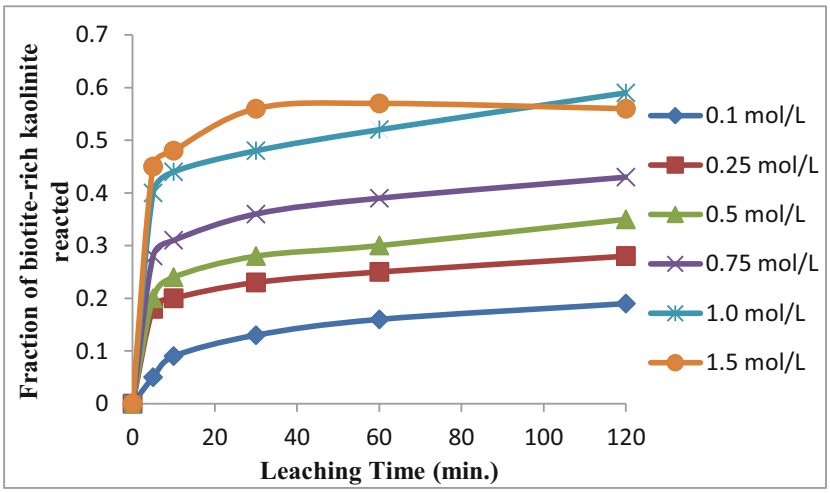

Fig. 2 Fraction of biotite-rich kaolinite ore reacted at different concentrations of oxalic acid

3.3 Leaching Investigations

3.3.1 Effect of Leachant Concentration

The effect of oxalic acid ($C_2H_2O_4$) concentration on the extent of the biotite-rich kaolinite ore reacted was studied within an acid range of 0.1–1.5 mol/L at 55 °C. The amounts of the ore reacted with different oxalic acid concentrations at different leaching times are shown in Fig. 2.

Conditions:[$C_2H_2O_4$] = 0.1–1.5 mol/L, reaction temperature = 55 °C, particle size = −75 +45 μm.

As summarized in Fig. 2, the fraction of the ore reacted increased with increasing acid concentration. For example, with 0.1 mol/L and 1.0 mol/L $C_2H_2O_4$ solution, the extent of ore dissolution reached 19.0% and 59.0% within 120 min at 55 °C. However, the extent of the ore dissolution decreased from 59.0% to 56.0% with increasing lixiviant concentration from 1.0 mol/L to 1.5 mol/L at defined conditions. The possible reason for this decrease in the amount of the ore reacted could be precipitation phenomena at higher oxalic acid strengths [23, 24]. Thus, 1.0 mol/L $C_2H_2O_4$ was recorded as optimal leachant concentration and was subsequently used for optimization of other leaching parameters in this study.

3.3.2 Effect of Reaction Temperature

In this section, the experiments were carried out in a temperature range of 25–75 °C using the ore sample with the finest particle size (−75 +45 μm) and 1.0 mol/L oxalic acid concentration at a moderate rate of stirring (300 rpm). An appropriate plot was made from the experimental data, as summarized in Fig. 3.

Figure 3 shows that the extent of the ore reacted increased with increasing reaction temperature. For example, the extent of the ore dissolution for 25 °C and 75 °C was 27.0% and 92.0% within 120 min, respectively. The fraction of the ore reacted was more sensitive to reaction temperature between 65 and 75 °C, as there could be a rapid formation of layers on the particle surface, altering leachant penetration to the reactive region at lower temperatures [25].

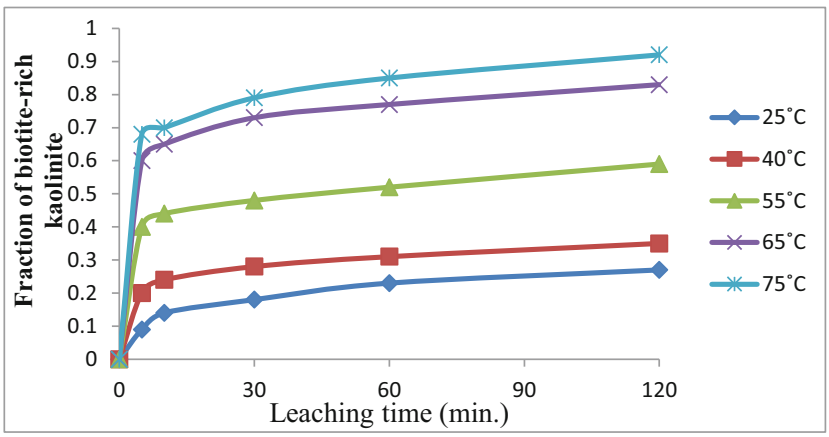

Fig. 3 Effect of reaction temperature on the fraction of ore reacted. *Conditions:*[$C_2H_2O_4$] = 0.1–1.0 mol/L, reaction temperature = 25 – 75 °C, particle size = −75 +45 μm

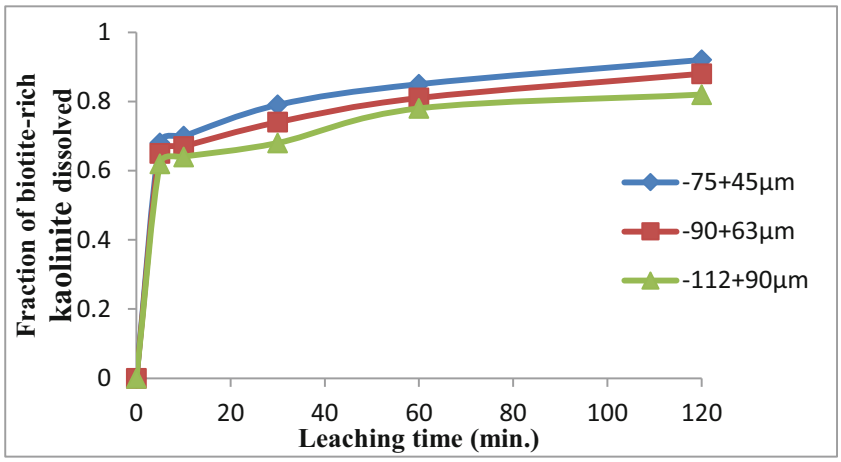

Fig. 4 Fraction of kaolinite reacted against leaching time for different particle sizes

3.3.3 Effect of Particle Size

The experiments were conducted using three different particle size ranges, namely −75 +45 μm, −90 +63 μm, and − 112 + 90 μm, while two other parameters were kept constant: temperature at 75 °C and oxalic acid concentration at 1.0 mol/L. The effect of particle size on the fraction of ore reacted is illustrated in Fig. 4, which demonstrates that the dissolution rate increased with decreasing ore particle size under the optimal conditions.

Figure 4 demonstrates that with −75 +45 μm, −90 + 63 μm and − 112 +90 μm, the fraction of the biotite-rich kaolinite ore reacted at 75 °C with 1.0 mol/L $C_2H_2O_4$ solution was 92.0%, 88.0% and 82.3% within 120 min, respectively. It is obvious that the ore with finest particle size, which was assumed to have a larger surface area, reacted significantly more than other two particle sizes. These results confirm those of other studies showing that increased particle size resulted in a decrease in the dissolution rate, which was attributed to the decrease in contact mass with the larger particle size [26, 27]. At optimal conditions (75 °C, 1.0 mol/L $C_2H_2O_4$), the metal species in the leach solution for the dissolution of 10 g/L ore during 120 min reaction gave 1564.7 mg/L Al^{3+}, 123.4 mg/L Fe^{3+}, 70 mg/L Mn^{2+} and 17.6 mg/L Ti^{2+}, respectively. Other metal ion species detected (Ca, Mg) occurred in low to trace amounts (≤1 mg/L). The treatment and purification of this solution with appropriate extracting agents will be reported in due course.

3.4 Discussion

3.4.1 Kinetic Analysis

Following the above dissolution data, the possible pathways for elucidating the exact mechanism for the defined ore leaching reactions are often based on key factors including stoichiometry, rate constant, reaction order, activation energy and data correlation [28]. In heterogeneous leaching reactions, for example, there are two prominent reaction steps on which the overall mechanism relies: film diffusion to the surface of the particle, and diffusion through the product layer.

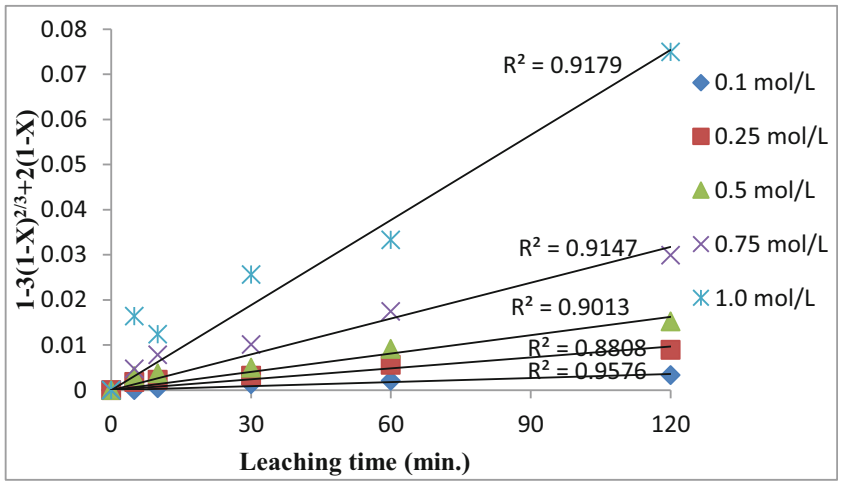

Fig. 5 Plots of $1-3(1-X)^{2/3}+2(1-X)$ versus leaching time as a function of leaching time. *Conditions:* same as in Fig. 2

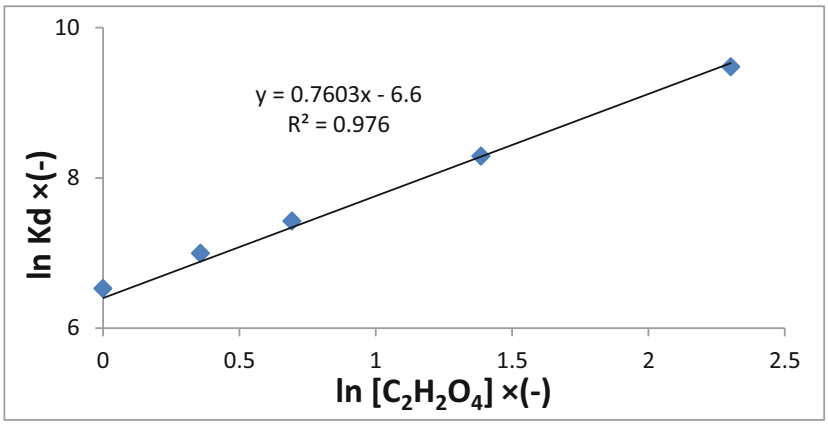

Fig. 6 Plot of lnkd against $\ln[H_3PO_4]$. *Conditions:* same as in Fig. 4

However, irrespective of the dissolution pathway during heterogeneous processes, several kinetic model mechanisms have been mobilized to better understand the defined dissolution pathways [29, 30]. Thus, in this study, attempts were made to subject all experimental data obtained (runs at different reaction temperatures and acid concentration) to a shrinking core model (SCM) mechanism used in solid-state reactions. The SCM assumes that the reaction products remaining in the solid phase form a layer of "ash" that encloses the unreacted core. The equations of the shrinking core model as previously proposed and used in this study can be expressed as [31]:

$$1-3(1-X)^{2/3}+2(1-X)=Kd.t \quad \text{(diffusion controlled process)} \tag{4}$$

$$1-(1-X)^{1/3}=Kc.t \quad \text{(chemical reaction controlled process)} \tag{5}$$

X is the fraction of biotite-rich kaolinite ore reacted, t is the reaction time, and Kd and Kc are the reaction rate constants. The dissolution data in Figs. 2, 3, and 4 were appropriately fitted into the shrinking core model Eqs. (4) and (5). It is important to note that the dissolution data fitted perfectly with model Eq. (4), with an average correlation (R^2) value of 0.9576 as compared to an R^2 value of 0.422 obtained with Eq. (5) testing. Therefore, the dissolution process by oxalic acid leachant in this study is apparently dominated by the diffusion-controlled mechanism, and Eq. (4) was applied. To estimate the reaction order, the dissolution data in Fig. 2 were linearized with Eq. (4) as summarized in Fig. 5.

The diffusion rate constant (Kd) obtained from Eq. (4) was used to construct the Arrhenius plot, lnKd versus ln $[C_2H_2O_4]$. The derived slope equivalent of 0.7603 from Fig. 6, with a correlation coefficient of 0.976, reveals a first-order dissolution relationship at defined leachant concentrations.

The dissolution data in Fig. 3 were also linearized using Eq. (4) to obtain the following plot (Fig. 7).

The slopes of Fig. 7 were assumed to be equal to the inverse of the completion time for the reaction of the entire particle; therefore, at 75 °C, 92.0% dissolution was achieved within a residence time of 2 h. Hence, to obtain the same yield at 25 °C, the ore dissolution would require about 40 h of treatment.

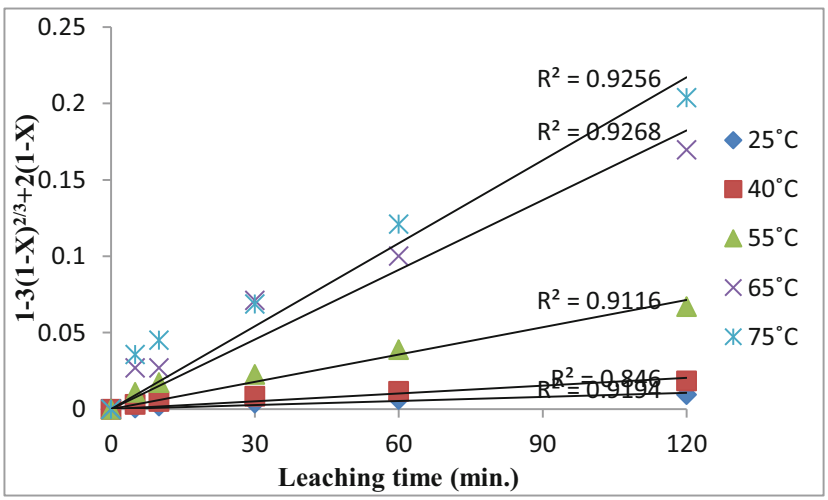

Fig. 7 Plot of $1-3(1-X)^{2/3}+2(1-X)$ versus leaching time at different temperatures. *Conditions:* same as in Fig. 3

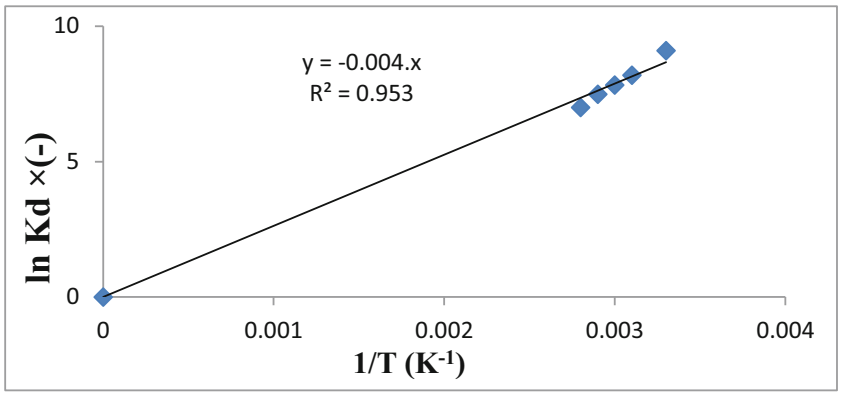

Fig. 8 Arrhenius relation ln Kd versus 1/T (K^{-1})

Table 1 Reported activation energies of kaolinite ore processing by acid leaching from different sources

Origin	Activation energy (Ea), $kJmol^{-1}$	Proposed mechanism	References
Zacatecas (Mexico)	46.32	Chemical control	Martinez-Luevanos et al., 2011 [33]
Mongolia (China)	78.3	Chemical control	Feng et al., 2014 [34]
Egbeda (Nigeria)	41.34	Chemical control	Baba et al., 2015 [16]
Nane Didan Bungudu (Nigeria)	33.2	Diffusion control	This study

In Fig. 8, appropriate plots of lnK versus 1/T were constructed, and the apparent activation energy was obtained from the following relations:

$$K = A\exp\left(-\frac{Ea}{RT}\right), \tag{6}$$

linearized as:

$$lnK = lnA + \left(-\frac{Ea}{R}\right)\frac{1}{T}, \tag{7}$$

K is the reaction rate constant, A is the pre-exponential factor, Ea is the activation energy (kJ/mol), R is the gas constant, and T is the reaction temperature.

The activation energy for the dissolution of the biotite-rich kaolinite ore derived from Fig. 8 gave 33.2 kJ/mol, which supported the proposed mechanism. From the literature, higher activation energy (≥ 40 kJ/mol) implies that the mechanism is controlled by a chemical reaction, while lower activation energy (≤ 40 kJ/mol) suggests a diffusion reaction as the rate-controlling step [32]. Thus, it is appropriate to state that the dissolution pathway in this study followed a diffusion control mechanism. Activation energy values of various kaolinite varieties from different sources reported by other authors are summarized in Table 1.

One can clearly see in Table 1 that the kaolinite ore sourced from Nane Didan Bungudu (northern Nigeria) requires lower energy for upgrade to industrial added value compared with

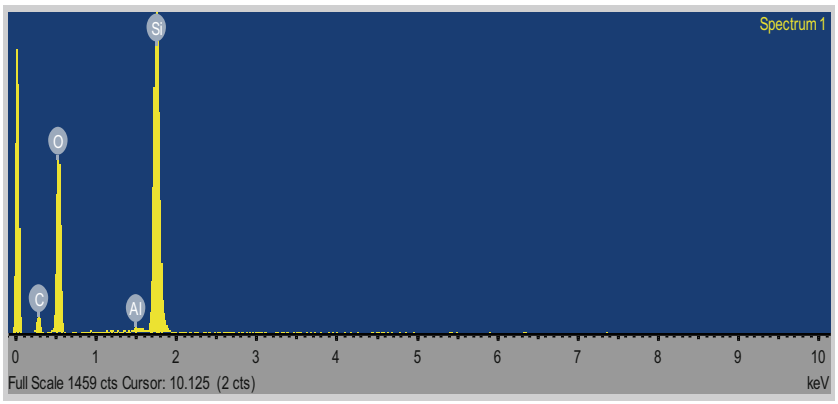

Fig. 9 The EDS spectrum of the $C_2H_2O_4$-leached residue of the biotite-rich kaolinite at optimal conditions

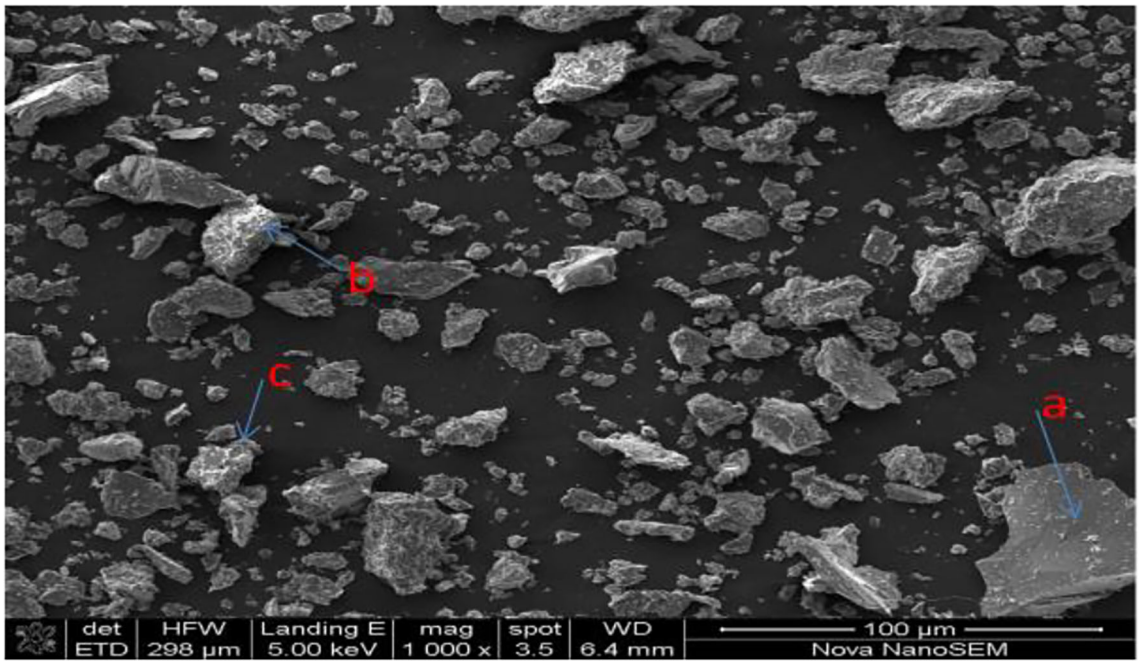

Fig. 10 The SEM micrograph of the $C_2H_2O_4$-leached residue of the biotite-rich kaolinite ore at optimal conditions

ore sourced from the western part of the country [16] and with other ores sourced from different countries.

3.4.2 Residual Product Analysis

The elemental composition of the residual product at optimal conditions demonstrated in Fig. 9 by EDS gave Al (5.82%), Si (20.25%), O (53.04%) and C (20.88%). This result showed that the undissolved species at optimal leaching examined by XRD contain siliceous impurities: SiO_2 (45-209-1788) with traces of aluminum species (≤1%) detected.

The SEM pattern of the acid-leached residue at optimal conditions (75 °C, 1.0 mol/L $C_2H_2O_4$, −75 +45 μm) shown in Fig. 10 reveals that the unreacted product exhibits a vermicular shape with irregular bulk edges and surfaces that are much smoother compared with the parent ore (Fig. 1) [35]. The surface characteristics of the residual product at optimal conditions are summarized in Fig. 10, indicated as *a*, *b*, and *c* spots, which confirmed the presence of Al, Si and O, respectively [15].

4 Conclusion

The present study examined the dissolution rate of biotite-rich kaolinite ore using $C_2H_2O_4$ solution as the leachant. The effect of reaction temperature, leachant concentration and particle size on the extent of the ore dissolution was investigated. The results obtained suggest that the dissolution rate increased significantly with leachant concentration and reaction temperature, and decreased with increasing particle size. At optimal conditions, 92.0% of the initial 10 g/L ore reacted within 120 min, and the unleached product revealed by XRD and EDS analyses contained siliceous impurities that could serve as a by-product for some industries.

The dissolution data were also analyzed by shrinking core models (SCM) and found to follow the diffusion controlled reaction. The calculated activation energy of 33.2 kJ/mol supported the proposed reaction mechanism. Hence, the results of this investigation reveal that oxalic acid leachant is effective for upgrading a biotite-rich kaolinite ore of Nigerian origin for industrial value. The purification of the leachate obtained at optimal leaching in this study will be reported in due course.

Acknowledgements The authors are grateful to Miranda Waldron of the Centre for Imaging & Analysis, University of Cape Town, South Africa for assisting with SEM and EDS analyses.

Compliance with Ethical Standards

Conflict of Interest On behalf of all authors, the corresponding author states that there is no conflict of interest.

References

1. Gajam SY, Raghavan S (1985) A kinetic model for the hydrochloric acid leaching of kaolinite clay in the presence of fluoride ions. Hydrometallurgy 15(2):143–158
2. Wu CY, Yu HF, Zhang HF (2012) Extraction of aluminium by pressure acid-leaching method from coal fly ash. Trans Nonferrous Metals Soc China 22(9):2282–2288

3. Matjie RH, Bunt JR, Van-Heerden JHP (2005) Extraction of alumina from coal fly ash generated from a selected low rank bituminous South African coal. Miner Eng 18(3):299–310
4. Turhan Y, Dogan AM (2010) Poly(vinyl chloride)/kaolinite nanocomposites: characterization and thermal and optical properties. Ind Eng Chem Res 49:1503–1513
5. Hamzaoui R, Muslim F, Guessasma S, Bennabi A, Guillin J (2015) Structural and thermal behavior of proclay kaolinite using high energy ball milling process. Powder Technol 271:228–237
6. Ptacek P, Opravil T, Soukali F, Wasserbauer J, Masiko J, Baracek J (2013) The influence of structure order on the kinetics of dehydroxylation of kaolinite. J Eur Ceram Soc 33:2793–2799
7. Lu M, Xia G, Zhang X (2017) Refinement of industrial kaolin by removal of iron-bearing impurities using thiourea dioxide under mechanical activation. Appl Clay Sci 141:192–197
8. Taran M, Aghaie E (2015) Designing and optimization of separation process of iron impurities from kaolin by oxalic acid in bench-scale stirred-tank reactor. Appl Clay Sci 107:109–116
9. Cao W, Xia C, Lu M, Huang H, Xu Y (2016) Iron removal from kaolin using binuclear rare earth complex activated thiourea dioxide. Appl Clay Sci 126:63–67
10. Michaela T, Jonas T, Kristina C, Vlastimil M, Katerina MK, Jana S (2014) The stability of photoactive kaolinite/TiO2 composite. Composites 67:262–262
11. Cameselle C, Ricart MT, Nunez MJ, Lema JM (2003) Iron removal from kaolin. Comparison between "in situ" and "two-stage" bioleaching processes. Hydrometallurgy 68:97–105
12. Gonzalez JA, Del JA, Ruiz C (2006) Bioleaching of kaolins and clays by chlorination of iron and titanium. Appl Clay Sci 33:219–229
13. Hosseini MR, Pazouki M, Ranjbar M, Habibian M (2007) Bioleaching of iron from highly contaminated kaolin clay by *Aspergillus niger*. Appl Clay Sci 33:251–257
14. Thurlow C (2001) China clay from Cornwall and Devon-The Modern China Clay Industry, Cornish Hillside publication, St. Austell, Cornwall. In: Lu M, Xia G, Zhang X (2017) Refinement of industrial kaolin by removal of iron-bearing impurities using thiourea dioxide under mechanical activation. Applied Clay Science, 141, p 192-197
15. Liu W, Tang C, He J, Yang J, Yang S (2010) Dissolution kinetics of low grade complex copper ore in ammonia-ammonium chloride solution. Trans Nonferrous Metals Soc China 20:910–917
16. Baba AA, Mosobalaje MA, Ibrahim AS, Girigisu S, Eletta OAA, Aluko FI, Adekola FA (2015) Bleaching of a Nigerian kaolin by oxalic acid leaching. J Chem Technol Metall 50(5):623–630
17. Velho JAGL, Gomes CF (1991) Characterization of Portuguese kaolins for the paper industry: beneficiation through new delamination techniques. Appl Clay Sci 6:155–170
18. Lima PEA, Angélica RS, Neves RF (2014) Dissolution kinetics of metakaolin in sulfuric acid: comparison between heterogeneous and homogeneous reaction methods. Appl Clay Sci 88-89:159–162
19. Hernandez RA, Garcia FL, Hernandez LE, Luevanos AM (2012) Iron removal from kaolinite clay by leaching to obtain whiteness index. 3rd Congress on Materials Science and Engineering (CNCIM-Mexico 2012), IOP Conf. Series: Mat. Sci. Eng., 45, p 1-5
20. Altiokka MR, Akalin H, Melek N, Akyalcin S (2010) Investigation of the dissolution kinetics of meta-kaolin in H_2SO_4 solution. Ind Eng Chem Res 49:12379–12382
21. Sathy C, Ramaswamy S (2007) Investigation on a gray kaolin from south east India. Appl Clay Sci 37:32–46
22. Raji MA (2017) Purification of Biotite-rich Kaolinite mineral for Industrial Applications, M.Sc. Thesis, Department of Industrial Chemistry, University of Ilorin, Nigeria, p 1-165
23. Mahi P, Livingston WR, Rogers DA, Chapman RJ, Bailey NT (1991) The use of coal spoils as feed materials for alumina recovery by acid leaching routes. Part 6: the purification and crystallization of chloride and chloride/fluoride leach liquors by HCl gasprecipitation. Hydrometallurgy 26:75–91
24. Cui HX, Cheng WT, Guo YX, Cheng FQ (2013) Study of the solubility of $AlCl_3.6H_2O$ in several chlorides systems. Ind Inorg Salt 45(5):12–15
25. Li C, Yanxia G, Xuming W, Zhiping D, Fangqin C (2015) Dissolution kinetics of aluminium and iron from coal mining waste by hydrochloric acid. Chin J Chem Eng 23:590–596
26. Hursit M, Lacin O, Sarac H (2009) Dissolution kinetics of smithsonite ore as an alternative zinc source with an organic leach reagent. J Taiwan Inst Chem Eng 97:6–12
27. Santos FM, Pina FM, Porcaro PS, Oliveira R, Silva AV, Leão VA (2010) The kinetics of zinc silicate leaching in sodium hydroxide. Hydrometallurgy 102:43–49
28. Moore, J. (1981) Chemical Metallurgy. Butterworth and Co, England, In: MacCarthy J, Nosrati A, Skinner W, Addai-Mensah J (2015) Effect of mineralogy and temperature on atmospheric acid leaching and rheological behavior of metal oxide and clay mineral dispersions. Powder Technology, 286, p 420-430
29. Gbor PK, Ahmed IB, Jia CQ (2000) Behaviour of Co and Ni during aqueous sulphur dioxide leaching of nickel smelter slag. Hydrometallurgy 57:13–22
30. Levenspiel O (1999) Chemical reaction engineering. Wiley, New York
31. Cheng WP, Fu CH, Chen PH, Yu RF (2012) Dynamics of aluminum leaching from water purification sludge. J Hazard Mater 217–218:149–155
32. Brantley SL (1995) Kinetics of mineral dissolution, kinetics of water-rock interaction. Springer, Chapter, 5
33. Martínez-Luévanos A, Rodríguez-Delgado MG, Uribe-Salas A, Carrillo-Pedroza FR, Osuna-Alarcón JG (2011) Leaching kinetics of iron from low grade kaolin by oxalic acid solutions. Appl Clay Sci 51:473–477
34. Feng P, Xuchen L, Yun W, Shiwei C, Tizhuang W, Yan Y (2014) Synthesis and crystallization kinetics of ZSM-5 without organic template from coal-series kaolinite. Microporous Mesoporous Mater 184:134–140
35. Abd El-Moghny MW (2017) The nature, origin and distribution of kaolinite in the lower Paleozoic Naqus formation along western side of Gulf of Suez, Egypt. Nat Sci 15(2):49–61